Model of Gait Control in Parkinson's Disease and Prediction of Robotic Assistance

Clémence Vandamme, Virginie Otlet, Renaud Ronsse, *Member, IEEE*, and Frédéric Crevecoeur

***Abstract*— Gait variability of healthy adults exhibits Long-Range Autocorrelations (LRA), meaning that the stride interval at any time statistically depends on previous gait cycles; and this dependency spans over several hundreds of strides. Previous works have shown that this property is altered in patients with Parkinson's disease, such that their gait pattern corresponds to a more random process. Here, we adapted a model of gait control to interpret the reduction in LRA that characterized patients in a computational framework. Gait regulation was modeled as a Linear-Quadratic-Gaussian control problem where the objective was to maintain a fixed velocity through the coordinated regulation of stride duration and length. This objective offers a degree of redundancy in the way the controller can maintain a given velocity, resulting in the emergence of LRA. In this framework, the model suggested that patients exploited less the task redundancy, likely to compensate for an increased stride-to-stride variability. Furthermore, we used this model to predict the potential benefit of an active orthosis on the gait pattern of patients. The orthosis was embedded in the model as a low-pass filter on the series of stride parameters. We show in simulations that, with a suitable level of assistance, the orthosis could help patients recovering a gait pattern with LRA comparable to that of healthy controls. Assuming that the presence of LRA in a stride series is a marker of healthy gait control, our study provides a rationale for developing gait assistance technology to reduce the fall risk associated with Parkinson's disease.**

***Index Terms*— Fractal, gait analysis, optimal control, Parkinson's disease, robotic assistance.**

I. Introduction

GAIT, as many other physiologic signals, possesses a complex temporal organization. Indeed, the fluctuations from one stride to another, originally considered as random noise, display Long-Range Autocorrelations (LRA) [1]. It means that the fluctuation at any time statistically depends on remote previous cycles with a power-law relationship, revealing the existence of a long-term dependency in the locomotor system. The presence of a temporal correlation across consecutive strides is characterized by the Hurst exponent, a metric directly linked to the autocorrelation function and reflecting the degree of this autocorrelation [2].

This feature is considered to indicate the flexibility and adaptability of the locomotor system to external events. Clinically, its presence is often considered as a marker of health, while its alteration has been associated with different pathological conditions [3]. In particular, it has been shown that the presence of LRA in the series of consecutive stride durations of patients with Parkinson's Disease (PD) is decreased compared to healthy individuals [4], [5], and that this decrease becomes more pronounced as the disease progresses [6]. This indicates that these patients have a more random temporal organization of the stride series, which is associated with an increased risk of falling [7], and therefore decreases their quality of life.

The physiological origins of LRA in gait variability of a healthy population, as well as the reasons why these LRA are impacted in the PD population, remain unclear. Several models have been developed to understand the mechanisms governing the presence of LRA in inter-stride interval time series [8], [9], [10], [11]. Among those, some authors attribute the presence of LRA to the biomechanics of walking while others argue for a neural origin. Some studies demonstrated that LRA are partly under volitional control and evidenced the supra-spinal influence on the correlation structure, since gait [12] or cycling patterns [13] become less correlated when guided with a metronome. Likewise, the early stages of PD are associated with a decline in LRA while biomechanics at this stage can be considered unaltered. Therefore, we assumed here a neural origin for the presence of LRA. The present paper looked specifically at the model of Dingwell et al. [11], which reproduced gait variability in a healthy young population within the framework of stochastic optimal control, in a way that is independent of the biomechanical system. This model suggested that LRA emerge from the fact that humans exploit the task redundancy to regulate their velocity while walking.

Based on this model, we addressed the two following questions. First, we investigated whether and how the model could be adapted to simulate gait impairments experienced by PD patients for different stages of the disease. Second, the model was used to investigate the impact of a robotic device and, more specifically on the possibility of restoring

Manuscript received 5 July 2022; revised 28 December 2022; accepted 23 January 2023. Date of publication 14 February 2023; date of current version 24 February 2023. This study was supported by the UCLouvain (Action de Recherche Concerté "coAction"). *(Corresponding author: Frédéric Crevecoeur.)*

Clémence Vandamme and Frédéric Crevecoeur are with the Louvain Bionics, Institute of Information and Communication Technologies, Electronics and Applied Mathematics, UCLouvain, 1348 Louvain-la-Neuve, Belgium, and also with the Institute of Neurosciences, UCLouvain, 1200 Woluwé-Saint-Lambert, Belgium (e-mail: frederic.crevecoeur@uclouvain.be).

Virginie Otlet is with the Louvain Bionics, Institute of Mechanics, Materials, and Civil Engineering, UCLouvain, 1348 Louvain-la-Neuve, Belgium.

Renaud Ronsse is with the Louvain Bionics, Institute of Mechanics, Materials, and Civil Engineering, UCLouvain, 1348 Louvain-la-Neuve, Belgium, and also with the Institute of Neurosciences, UCLouvain, 1200 Woluwé-Saint-Lambert, Belgium.

Digital Object Identifier 10.1109/TNSRE.2023.3245286

the presence of LRA in the series of stride parameters. Indeed, robot-assisted gait training has shown promising effects on the gait of PD patients. Some studies showed improvements of gait parameters such as velocity, endurance, stride length and duration, cadence, and balance [14]. Other advances in the development of assisted gait include studies on the effect of oscillator-based walking assistance on the presence of LRA [15], based on the Super Central Pattern Generator model described in [8].

In this paper, we demonstrate that gait parameters in Parkinson's disease can result from an augmentation of stride-to-stride regulation used to mitigate the impact of noise. Moreover, the decline in LRA in patients could be a consequence of a relative inability to exploit the task redundancy. It is also demonstrated that an oscillator-based robotic assistance, included in the model as a low-pass filter, could restore the presence of LRA in simulated time series of stride durations. These results provide theoretical support for developing gait assistance technology for patients with a view towards reducing the risk associated with falling as the disease progresses.

II. Materials and Methods

A. Data

The experimental stride series of healthy subjects from [11] were re-used to validate the model. The dataset was composed of 34 stride sequences characterized by the stride duration (T), length (L) and velocity (S). The experiment involved 17 healthy young adults. Each participant was asked to walk on a treadmill for 5 minutes at a self-selected speed. Each participant completed two trials with a 2-minute break in between. Series length ranged from 248 to 309 strides. Mean values, standard deviation and Hurst exponent of all series (T, L and S) were averaged across participants and the 95% confidence intervals were computed, assuming a normal distribution ($CI = Mean \pm 1.96 * SD$).

In addition, data of PD patients were collected by Warlop et al. [6] and also incorporated in the present analyses. This study included 20 patients with PD, who were asked to walk overground for 10 minutes at a self-selected speed. For each patient, stride durations (T) were extracted from series of 512 strides. The dataset included the stage of the disease of each patient, assessed using the modified Hoehn & Yahr scale (H&Y), here ranging from 1 to 3. These scores monitor the progression of the disease based on a clinical evaluation of motor performances. The H&Y evaluation includes a balance assessment, the severity of tremor, bradykinesia and rigidity, and whether symptoms are unilateral or bilateral. Unlike healthy participants' data, this dataset only contained the series of stride durations, and not stride lengths. Again, the mean, standard deviation, and Hurst exponent were computed. Then, a standard least-square regression line was drawn to model the evolution of each variable (standard deviation and Hurst exponent) as a function of the disease progression, captured by the H&Y index. The Spearman's correlation coefficient was used to assess the relationship between this index and both the stride variability and the stride persistence. The level of significance was set to $p < 0.05$.

B. Assessment of the Long-Range Autocorrelation

The Hurst exponents, noted H, were computed with the Adaptive Fractal Analysis (AFA), a method described by Riley and colleagues [16] and recently recommended for stride time fractal exponents [17]. Briefly, the AFA consists in identifying smooth trends signals from a time series. The process is repeated for trends of different timescales and the residuals of each fit are reported against the corresponding timescale. The analysis of the scaling of the residuals as a function of the timescales gives the Hurst exponent of the time series. If $0 \leq H < 0.5$, the series is said to be anti-persistent, meaning that it exhibits negative LRA. If $H = 0.5$, the series corresponds to random fluctuations around its mean (white noise). If $0.5 < H \leq 1$, the series is persistent, or has positive LRA. The Hurst exponent relates to the fractional Brownian motion model and is by definition restricted within the interval]0,1[[18]. Other notations exist, like the scaling exponent α, which simply extends the definition of H to values larger than 1 [19]. This refers to non-stationary series, a case that was not encountered in this paper.

The AFA is similar to the Detrended Fluctuation Analysis (DFA) [20], more commonly used in the evaluation of LRA, as both algorithms quantify the residuals of fits computed with different sizes of time window. The main difference is that AFA identifies globally smooth fits by combining overlapping windows and is therefore more robust to non-stationarities [21].

C. Gait Model for Young and Healthy Population

The model developed to reproduce gait variability of PD patients and predict the impact of a robotic assistance was based on the model previously published by Dingwell and colleagues [11], capturing gait variability in a healthy and young population. The model aimed at describing the inter-stride dynamics resulting from a regulation derived in the context of Linear-Quadratic-Gaussian (LQG) control. Strides were fully characterized by their length (L) and duration (T) from which the speed (S) was derived ($S = \frac{L}{T}$). Through a discrete system, these stride features were updated iteratively:

$$x_{n+1} = x_n + u(x_n) + N_n u(x_n) + \eta_n \quad (1)$$

where x_n is the state vector, composed of the duration T_n and length L_n of stride n. The term $u(x_n)$ is the motor command and $N_n u(x_n)$ represents a command-dependent noise, with N being a diagonal matrix. Finally, η is an additive noise vector. Both η and the diagonal of N are zero-mean, gaussian random variables with covariance matrix equal to $\mathrm{diag}[\sigma_1^2\ \sigma_2^2]$.

The command was determined by a controller, which regulated stride variability resulting from internal and external sources of noise according to a behavioral goal, i.e. keeping a constant velocity v (either strictly fixed by a treadmill or intrinsically selected by the walker based on their own preference). This means that the following equation should hold at each step: $L_n - vT_n = 0$. This task introduced redundancy as there is an infinite amount of combinations of T_n and L_n that satisfy this relationship. These combinations form a straight line in the plane T, L, called the Goal Equivalent Manifold (GEM).

Along this redundant dimension, one pair of T and L might be naturally preferred by the participant for biomechanical reasons (length of the legs, inertia, etc.). This pair was referred to as the Preferred Operating Point (POP), corresponding to $T^*$and L^*. When noise disturbances push the state away from the POP, it is possible that locally, the optimal correction is to drive the system towards the GEM and not necessarily to the POP. To capture this, the model used the following cost-function for each step:

$$C = \alpha e^2 + \beta p^2 + \gamma u_1^2 + \delta u_2^2. \tag{2}$$

The first term penalizes the error on the velocity, with $e^2 = (L - vT)^2$. The second term concerns the distance from the POP, with $p^2 = (T-T^*)^2+(L-L^*)^2$. Then, the last two terms penalize the effort made to reduce these errors; u_1 (resp. u_2) being relative to the correction applied to the stride duration (resp. stride length). The parameters α, β, γ, and δ reflect the relative importance of the cost of each error term. The weights α and β correspond to the level of regulation applied respectively to the stride velocity and to the POP, with respect to the energetic cost that this regulation requires and that is quantified by the parameters γ and δ.

Finding the optimal command is a classic LQG control problem. We used the infinite horizon formulation as both the system and the cost are time-invariant. Moreover, the state was considered to be fully observable. The LQG framework provides a closed loop solution to the optimal control problem. The command is optimal in the sense that it minimizes the expected value of a quadratic cost criterion (Eq. 2) and is a linear function of the state (feedback gains). Details about the derivation of the optimal controller are provided in [22].

A schematic representation of the model is provided in Fig. 1 (top line). The first box is the controller, capturing the Central Nervous System. It takes as input the current state of the walker (i.e., the stride duration T and the stride length L) and their goal, in terms of stride length and stride duration (whose combination gives the targeted velocity). Considering these two inputs, the controller sends a command to the second box that captures the impact of the system, resulting in the next state.

We used a noise level of $\sigma_1 = 0.011$ (relative to T_n) and $\sigma_2 = 0.017$ (relative to L_n). The weights of the cost function were set to $\alpha = 30$, $\beta = 1$ and $\gamma = \delta = 10$. Finally, the target velocity was $v = 1.21$ [$\frac{m}{s}$], with $T^* = 1.105$ [s] and $L^* = vT^*$ [m]. These parameters allow the simulation of walking series of an average participant but do not model the variability of speeds adopted by different participants.

To validate the model, a total of 34 series of 512 strides were simulated and their features were compared to the experimental data. Each stride series was described by three series of inter-stride durations, lengths and velocities. The mean, standard deviation, and Hurst exponent of each series were computed. These values were then averaged over the 34 strides simulations and 95% confidence intervals were computed, as defined above.

D. Model Adaptations to Parkinson's Disease and Robotic Assistance

1) Parkinson's Disease: The model was adapted by tuning two parameters selected to reproduce the evolution of gait impairments with PD. To reproduce the increasing variability of inter-strides durations, the noise level of the system was increased (i.e. η in Eq. 1). The parameter σ_1, which is the variance of the noise impacting stride duration, was determined by fitting the experimental data. Then, assuming a similar variability increase of inter-stride length, σ_2 was multiplied by the same factor. To reflect the reduced Hurst exponent of patients, the weights of the cost function (Eq. 2) were also manipulated, in particular β, the weight penalizing deviations away from the POP. Again, this parameter was fitted to best reproduce the changes observed in the series of stride durations but impacted the persistence of the series of stride lengths as well. The tuning of parameters β and η was performed jointly because β affected both the variability and the persistence (i.e. the Hurst exponent) in the stride series. The model calibration was performed by testing all possible pairs of parameters ($1 < \beta < 35$ and $0.011 < \sigma_1 < 0.044$) and by selecting the parameters that best fitted the Hurst exponent and the variability of the experimental series of stride durations of 20 PD patients, according to a least-square fitting.

In Fig. 1, these changes are illustrated by an increased noise signal added to the motor command. The change of control strategy occurred in the Central Nervous System, where the weight β was impacted, reflecting a more pronounced tendency to regulate stride variables around the POP.

2) Effects of a Robotic Assistance: Robot-assisted gait training has shown promising effects on gait of PD patients [14]. Current studies have used adaptive oscillators in assistance [23], which resulted in a net effect on the discrete time model comparable with a low-pass filter. Indeed, adaptive oscillators learn the feature of the user's gait and tend to maintain them equal to what they used to be during the preceding cycles, by means of a soft and adaptive robotic assistance. As this has not been tested on PD patients yet, this study aimed to model the impact of such an assistance on the LRA of patients. The assistance was added to the system dynamics as follows:

$$\begin{aligned} x_{n+1} &= x_n + u(x_n) + N_n u(x_n) + \eta_n - \lambda(x_{n+1} - x_n) \\ \Leftrightarrow x_{n+1} &= x_n + (1+\lambda)^{-1}(u(x_n) + N_n u(x_n) + \eta_n), \\ \text{with } \lambda &= \begin{bmatrix} \lambda_1 & 0 \\ 0 & \lambda_2 \end{bmatrix}. \end{aligned} \tag{3}$$

The matrix λ represents the filter coefficient, which plays the role of time constant in the discrete time filter. It can be interpreted as the level of assistance of the orthosis, with λ_1 (resp. λ_2) the filter coefficient on the state variable T (resp. L). Higher coefficients correspond to higher degrees of assistance. The filter coefficients were tuned for every stage of the disease to recover a level of variability similar to that of control subjects (numerical values from Fig.2B). Then, the corresponding Hurst exponents were computed.

The orthosis and its controller thus intrinsically modify the dynamics of the user's "body", as it continuously interacts with

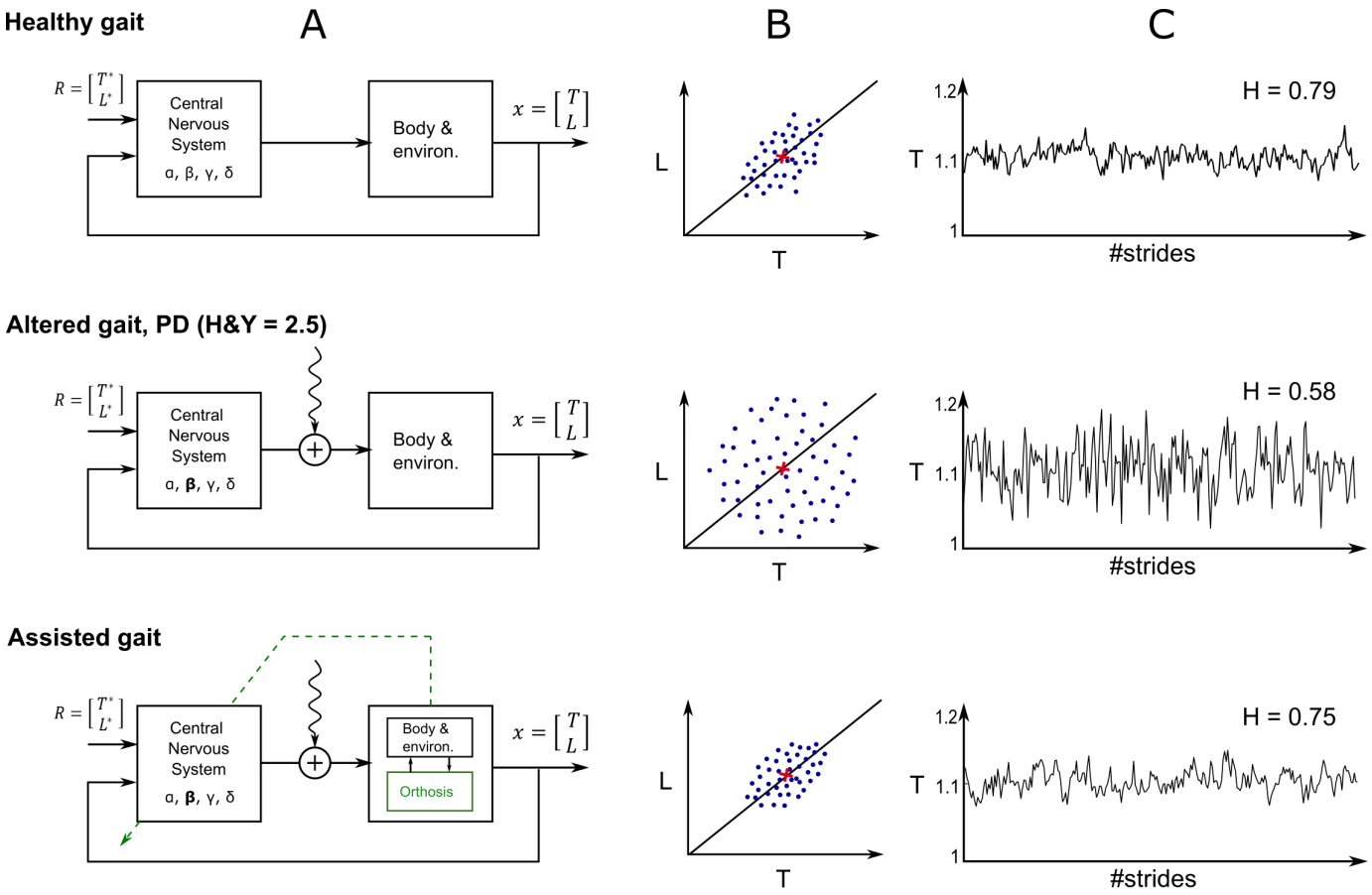

Fig. 1. (A, top to bottom) Schematic representation of the model for healthy gait, gait altered by Parkinson's disease, and gait altered by Parkinson's disease assisted by an orthosis driven by low-pass dynamics. (B) Simulated stride distribution (stride length "*L*" versus stride duration "*T*") around the goal equivalent manifold (black straight line) and the preferred operating point (red cross). (C) Example of simulated series of stride durations for each population (healthy - patients) and condition (assisted - unassisted) and their corresponding Hurst exponent (H).

it and affects stride generation accordingly. In Fig. 1, this is captured by embedding the orthosis in the "body + environment" block, i.e. the biomechanical system that is controlled by the central nervous system. However, it is unknown whether patients learn this new dynamic that includes the effect of the filter, i.e. of the assistive device. If they do, the controller uses Eq. 3 to derive the optimal motor command. This potential adaptation is captured by the green dashed line connecting both blocks, illustrating that the dynamic model is updated in the controller with knowledge of the filter. In contrast, patients who do not adapt their control will generate motor command considering Eq. 1 as a system model without the filter. Finally, a partial adaptation would consist in a controller that considers only a fraction of λ while computing the optimal command, resulting in a partial compensation for the filtering dynamics of the orthosis. The persistence of the time series from the two first conditions, referred as "adaptation" and "no adaptation", was compared across different values of λ used to lower the variability. The cost function remained unchanged (Eq. 2).

In addition, the model allows considering the possibility that the orthosis acts on the cadence only, on the stride length only, or on both. Three conditions were simulated: the orthosis filtered only the cadence ($\lambda_2 = 0$), only the stride length ($\lambda_1 = 0$) or both ($\lambda_1 = \lambda_2 > 0$), compared to no assistance at all ($\lambda_1 = \lambda_2 = 0$). For each situation, the Hurst exponents of the series of stride durations were reported.

Working code was made publicly available here: https://git.immc.ucl.ac.be/clevandamme/gait_model_pd.

III. Results

A. Healthy Gait

Each stride series was composed of a series of inter-stride durations, lengths and speeds. Each of them was analyzed in terms of mean, standard deviation and auto-correlation structure assessed based on an estimate of the Hurst exponent. The average results across 34 healthy participants (data from [11]) and simulations are reported in Fig. 2. For consistency with experimental data, the simulation results referred to series of 512 strides, but we verified that they were also valid for longer stride series (series of 1024 strides, data not shown). As expected, the means of simulated data matched exactly with values corresponding to the experimental series as they were used for calibrating the model. It can be reminded that the model did not intend to reproduce the inter-subjects' variability since all simulations were performed with the same velocity goal, and the same POP, whereas actual participants were asked to walk at their most natural speed, resulting in

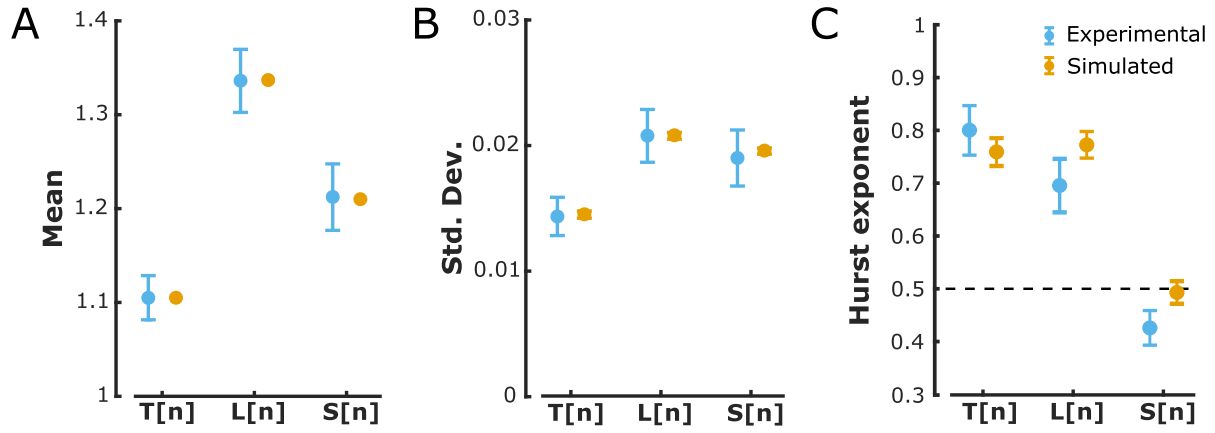

Fig. 2. (A) Mean stride durations ($T[n]$), lengths ($L[n]$) and speed ($S[n]$) for healthy subjects' data and simulated series. (B) Standard deviations of stride series ($T[n]$, $L[n]$ and $S[n]$. (C) Hurst exponent for $T[n]$, $L[n]$ and $S[n]$. Reported values result from an average of 34 experimental stride series from [11], compared to our simulations. Error bars represent the 95% confidence interval on these averages.

some variability across subjects. Note that for such standard parameter values, randomness in the time series produced higher levels of variability in the estimates of the Hurst exponents. The variability of the simulated series matched human data for T, L and S (Fig. 2B). While the variability of T and L could be directly manipulated through the parameters σ_1 and σ_2 (Eq. 1), the variability of S was a consequence of the combination of noise applied to T and L, as well as of the controller that regulated this velocity (α). We observed a relatively strong persistence in the experimental series of stride durations and lengths with values similar to those observed in overground walking experiments [24]. The model succeeded in reproducing a comparable persistence of T and L series, with mean Hurst exponents between 0.5 and 1 for both. Experimental data further suggested that velocity was slightly anti-persistent ($H < 0.5$), while the model simulated velocity series characterized by a Hurst exponent of 0.5, which can be interpreted as white noise. The observation that velocity was slightly anti-persistent was accommodated in the model previously proposed by [11] by considering a sub-optimal command to over-correct the errors on the velocity. We focused here on the formulation corresponding to the stochastic optimal control, which allowed capturing changes in the Hurst exponents of the series exhibiting changes in persistence, thus we do not model the anti-persistence explicitly. Furthermore,the anti-persistence of series of velocity may not generalize to overground walking since this has mostly been observed in treadmill studies [11], [25].

An example of simulated series of stride durations with characteristics as summarized in Fig. 2, is illustrated in Fig. 1 (top), as well as the strides distribution in the plane T, L. From Fig. 1B, we observe a narrow distribution along the GEM, meaning that each stride had a similar speed. In contrast, points were not constrained to remain in a close neighborhood of the POP, and had some freedom to move along the GEM.

B. Gait in Parkinson's Disease

The evolution of gait in PD patients according to disease severity is outlined in Fig. 3A. For each participant, the observed standard deviation and Hurst exponent of the series of inter-stride durations was plotted as a function of their clinical score obtained from the H&Y scale. Data of patients confirmed the previously observed significant increase in the standard deviation of series of strides durations (mean std $= 0.028 \pm 0.016$), compared to control subjects (0.014 ± 0.004, $t(50) = 4.62$, $p < 10^{-4}$). Experimental data also supported the decline of LRA in patients with PD ($H = 0.62 \pm 0.13$) compared to control subjects ($H = 0.8 \pm 0.13$, $t(50) = -4.71$, $p < 10^{-4}$).

Relating individual gait outcomes to disease severity illustrated the progressive impact of the disease on strides variability and persistence. The variability was correlated with the H&Y score with a Spearman's coefficient of 0.5. The regression was statistically significant ($R^2 = 0.22$, $F(1, 18) = 4.93$, $p = 0.04$). Concerning the persistence, the Spearman's coefficient was equal to -0.68. Again, the regression was statistically significant ($R^2 = 0.52$, $F(1, 18) = 19.86$, $p = 0.0003$). The disease stage was therefore clearly related to the variability of stride duration and to its temporal organization.

The linear regressions between the disease severity and the two variables of interest, namely the standard deviation and the Hurst exponent, were used as target values for the model simulations. To that purpose, two manipulations on the model were made. The first one was motivated by the observation that PD patients displayed larger inter-stride variability as described by the data presented in Fig. 3A. The simulation results and associated noise are represented in Fig. 3B and C respectively (top panel). The noise level increased linearly with the disease severity, but remained unchanged for patients with a H&Y score of 1. The adaptation of the noise parameter was performed jointly with the adjustment of the cost parameter β, which determined the penalty applied on errors on the POP. This manipulation aimed to reproduce the reduced LRA observed as the disease progresses. The Hurst exponents of simulated series and the corresponding β are reported in Fig. 3B and C (orange traces). The penalty β gradually increased to 30, a level comparable to the penalty applied on the velocity (α, Eq.2).

To illustrate the joint impact of the adaptation of noise and cost parameters, the green trace (Fig. 3B-C) represents an

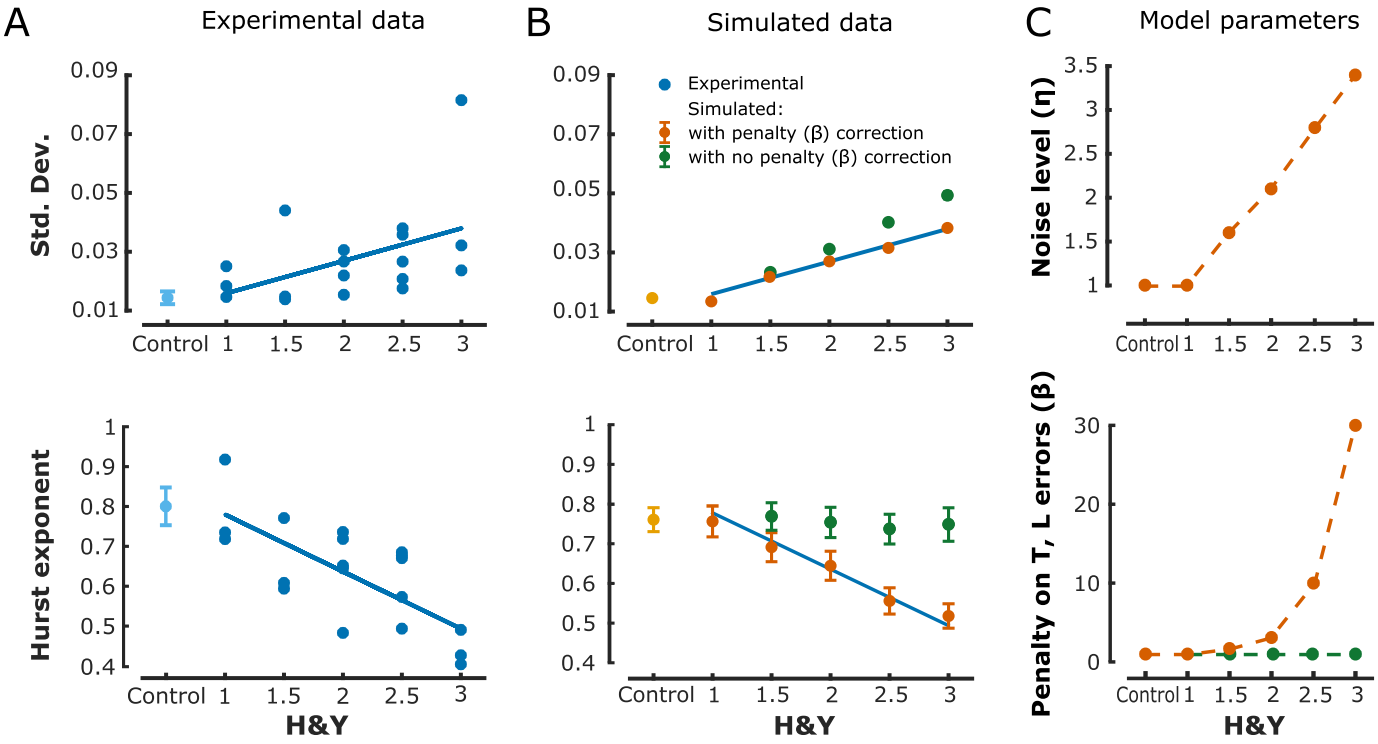

Fig. 3. (A) Individual standard deviation and Hurst exponent of series of stride durations of Parkinson's patients according to disease severity (assessed with the H&Y scale), compared to control group (light blue), data taken from [6]. (B) Mean standard deviation and Hurst exponent of 20 simulated series of stride durations according to disease severity. (C) Model parameters used to fit the stride characteristics of each disease stage (orange trace). The increasing level of noise in the system accounts for the higher variability in stride durations while a higher penalty away from the POP (T^* and L^*) is directly linked to a reduced Hurst exponent. In green, alternative set of parameters to illustrate the impact of the regulation on the POP.

alternative set of parameters, where only the noise level was modified. It highlights that, when the control was not adapted in response to the increase in noise variance, the increase in variability of the output series was in consequence more dramatic. For a H&Y of 3, the standard deviation increased by 35% when β remained fixed.

These results could not be obtained by changing other parameters. For $\beta = 1$, by dividing or multiplying α by 2, the Hurst exponent of T did not change. The impact was rather on the Hurst exponent of S, the series of stride velocities, which is not of interest here. Furthermore, the results of Fig. 3B were robust to small changes in the cost function. Changing β by $\pm 10\%$ had negligible effect on the standard deviation and the Hurst exponent. A typical simulated stride series and stride distribution matching the parameters of the empirical series obtained with PD patients is presented in Fig. 1B-C (middle). Strides were much more spread out, resulting from the increase in variability. The distribution otherwise aligned with the redundant axis of the task requirement became more circular around the POP, given that the weight on this part of the task increased.

C. Simulation of Robotic Assistance

To evaluate the potential impact of an orthosis, we simulated the same system and controller with the addition of a low-pass filter on the stride series as a first order model of the effect of a robotic device controlled by adaptive oscillators [23] on humans' gait dynamics. The impacts of the filter on the stride variability and on the LRA of the series are respectively described in Fig. 4A and 4B. Filter coefficients have been defined for each disease's stage to fit the variability of healthy gait. These are reported in Fig. 4C. Those coefficients differed depending on whether or not the patient had learned the new dynamics that included the effect of the filter (Eq. 3). In the first case, the patients adapted their control by considering the state transition dynamics as in Eq. 3, i.e. with the filter. In the second case, they acted as if there was no assistance and computed a command based on the system described in Eq. 1. The filter coefficients required to recover healthy levels of gait variability were higher if the patient did not adapt to the orthosis. Still, in both cases, the more the disease progresses (higher H&Y), the higher the level of assistance (higher λ). Lastly, in the model, it was not necessary to provide assistance for patients at the first stage of PD as their gait parameters matched those of the control group ($\lambda = 0$).

These values of λ produced strides series of mean standard deviations and mean Hurst exponents represented in Fig. 4A-B. Regardless of the simulated patient's adaptation, the robotic assistance reduced the stride variability and increased the Hurst exponent of series of stride durations, compared to non-assisted patients (solid blue line). The filter coefficients λ_1 and λ_2 were set in a way that the variability of assisted patients had the same value as that of healthy subjects. This is illustrated in Fig. 4A. As shown in Fig. 4B, the levels of persistence of patients adapting their control did not reach the reference value of control subjects for late stages of the

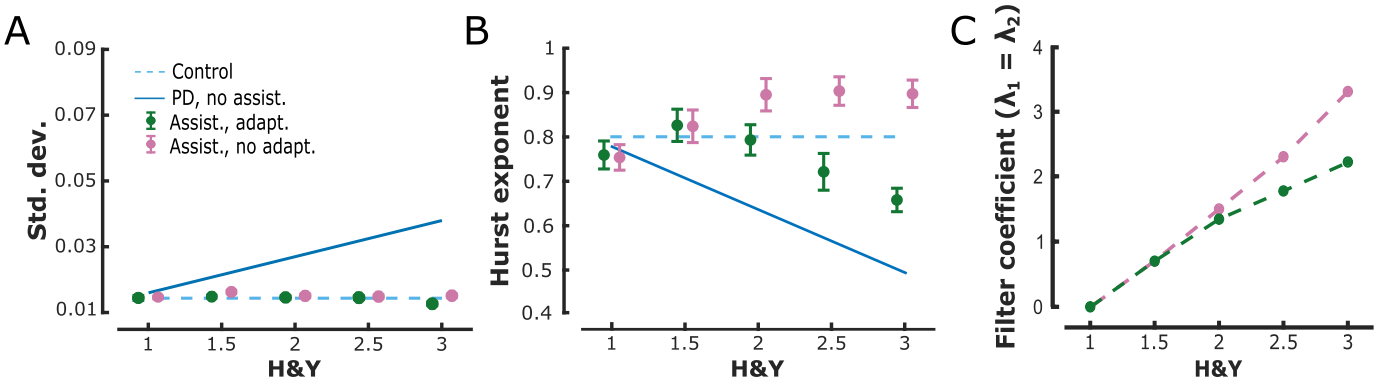

Fig. 4. Simulation of the effect of an orthosis on patients' series of inter-stride durations, both with (green) and without (pink) adaptation to the orthosis. Comparison of (A) the standard deviation and (B) the Hurst exponent of the simulated data to non-assisted patients and healthy subjects. (C) Filter coefficient applied to T and L required in both cases to reach levels of variability corresponding to healthy patients.

disease (H&Y $\geq$ 2.5). In contrast, if patients did not take into account the filtering, the Hurst exponents went beyond those of healthy subjects.

The model allows the investigation of another potential strategy, which would be to adjust the filter coefficient to match levels of persistence corresponding to those of healthy participants (dashed blue line). If the patients adapt to the robotic assistance, the filter coefficients must be further increased for patients with a H&Y $>$ 2. The variability is consequently further reduced and drops to $0.01[s]$ (-30%) for H&Y $= 3$. In the other case, if patients do not adapt their control, the filter coefficients must be lowered for patients with a H&Y $>$ 1.5. As a result, the variability reached a value of $0.018[s]$ ($+22\%$), for H&Y $= 3$. One of the simulations characterized in Fig. 4 is presented in Fig. 1B-C (bottom), illustrating the capabilities of the filter to recover stride series and stride distribution similar to those of healthy participants.

The foregoing simulations were derived by applying a filter to both T and L. We now present a comparison of the Hurst exponents of T, obtained with filters applied either only to the cadence, only to the stride length or to both (Fig. 5A), considering a full adaptation of patients. It appears that the persistence of T was not significantly increased when the simulated orthosis only acted on the length of the strides, compared to the Hurst exponents of simulated non-assisted patients. The Hurst exponent of T was only increased if the robotic assistance acted directly on the cadence, regardless of whether L was filtered or not. To illustrate this, an example of stride distribution for each situation is shown in Fig. 5B. The light and dark blue distributions correspond to those presented in Fig. 1B, middle and bottom respectively. In red, the filter was only applied to T, resulting in a distribution more constrained along the line $T = T^*$ with a small effect of the GEM, slightly tilting the distribution. In contrast, in green, it only filters L and strides are distributed along $L = L^*$. From this figure, we observe that a simple filter on the stride duration was sufficient to recover LRA compatible with series of healthy participants. However, a filter on the stride length, in addition to that applied to the cadence, was necessary to have a stride distribution more aligned with the redundant axis, like the stride distributions of healthy participants. Moreover, the series of stride lengths is most likely to be impacted by the disease too. Therefore, a filter would be necessary to strengthen the LRA of the series of stride lengths.

IV. Discussion

The purpose of this study was to develop a model capturing gait variability of PD patients to complement the current understanding of gait regulation in this population, with a particular emphasis on the decline of statistical persistence exhibited in stride-to-stride variability. A second objective was to study the effect of an oscillator-based robotic assistance on these patients' gait. For this purpose, we adapted the model capturing gait variability of healthy young adults, and added a low-pass filter representing the effect of the assistance on the time series of stride amplitudes and durations. According to the model developed in [11], the presence of LRA in gait variability emerged from a control strategy that first seeks to minimize velocity errors while only weakly limiting the deviations from the POP. In 2020, Kozlowska et al. [26] further supported this model by highlighting the strong coupling between the trends appearing in the series of stride duration and stride length, which corresponded to movements along the GEM. To capture the behavior of PD patients, the model was adapted by manipulating two parameters: the noise in the process dynamics was increased to reproduce the increase in variability of the stride series; and the cost parameter β was increased to reduce the statistical persistence of the series of stride durations. Considering these parameters adjusted to pathological gait, we showed that the addition of a low-pass filter - capturing the effect of an adaptive oscillator-based robotic assistance - had a positive impact on both the variability and the statistical persistence of stride series, and could restore values comparable to healthy groups.

The model developed in this study offers a novel interpretation of gait deficits in the PD population and suggests that patients adopted a different control strategy than healthy subjects. A first phenomenon known to be associated with the progression of the disease is the increase in stride-to-stride variability [27] that was directly captured by increasing the process noise. Then, we demonstrated that this variability, which must be undesirable beyond a certain level, can be

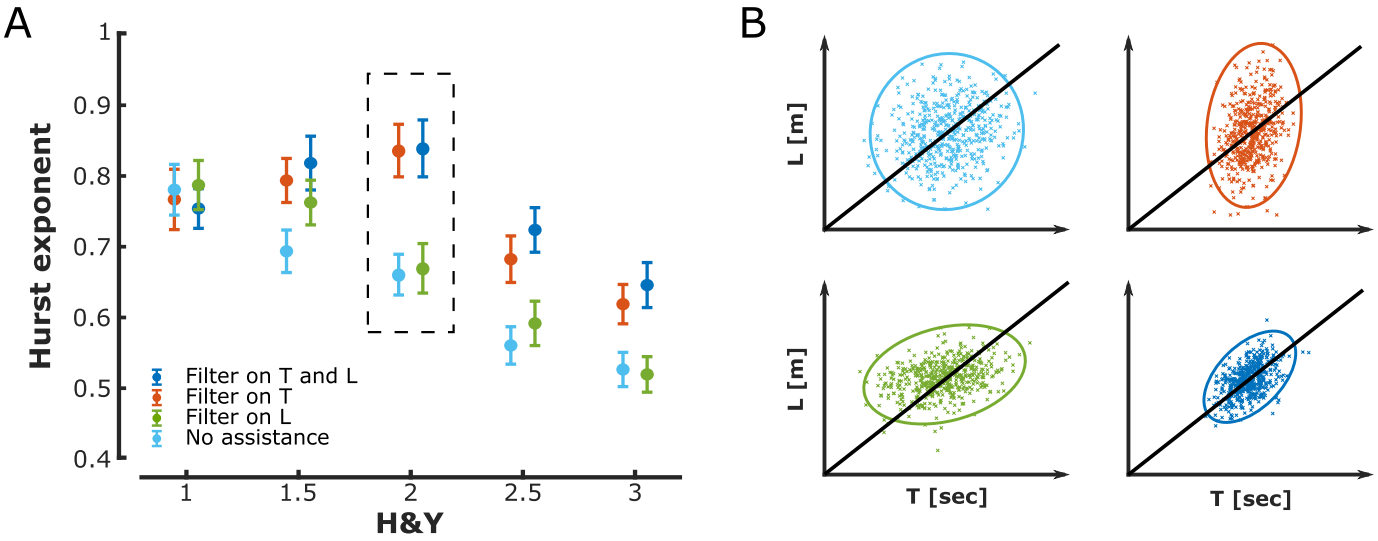

Fig. 5. (A) Mean Hurst exponent of simulated series stride durations according to disease severity with different kind of robotic assistance. The robotic assistance filters the stride duration T (red), the stride length L (green), both (dark blue), none (light blue). (B) For a H&Y of 2, the resulting stride distribution along the goal equivalent manifold for these 4 scenarios.

partially reduced by regulating gait parameters more strictly around the preferred operating point. This was achieved by increasing the cost of deviation from the POP captured in the model by the parameter β (Eq. 2). This regulation had a direct impact on the persistence of the series of stride durations. Not only gait parameters became more variable as a result of impairments in the sensorimotor system [7], [28], but the series also became more random, which in this framework, reflected a compensation strategy for the increased variability.

This hypothesis is in accordance with the fact that patients recruit more attentional resources while walking [29]. It has been shown that patients rely more on frontal-cortical mechanisms to support gait movement execution, due to defective basal ganglia mechanisms ensuring movement automaticity [30]. It is possible that patients recruit attentional resources to regulate not only the velocity, but also stride duration and stride length, which requires a conscious effort. The increased cognitive load associated with walking in PD patients is corroborated by the fact that strides variability is impacted when patients are instructed to execute another task while walking, such as a mental calculation [31]. A common interpretation of these findings is that the attentional resources are recruited for the dual task, and this impairs patients' control of gait. Our interpretation is in line with this idea and the model formalizes it in the context of stochastic optimal control. Our developments included an increased penalty on the deviation away from the POP, which is equivalent to assuming a more stringent regulation of inter-stride variability without exploiting the GEM. The latter likely incurs an attentional or cognitive load to control each individual stride.

This novel interpretation of gait deficits in PD patients is also in line with the use of therapies involving rhythmic cues. These therapies consist in providing external auditory cues adapting in real-time to the subject's gait rhythm so that the subject synchronizes their walking rhythm with this external rhythm. These studies showed an improvement in the presence of LRA to the level of healthy subjects [32], [33].

As an alternative to auditory stimulations, we explored potential benefits of robotic assistance based on adaptive oscillators with a net output on inter-stride time series comparable to a low-pass filter. We showed that such technology could restore healthy patterns of gait in PD patients, both in terms of standard deviation and statistical persistence. However, for a given set of parameters that one wishes to recover with the assistance, we found that the filter coefficients applied by the robot may depend on whether the patients adapt or not to the device. In practice, it is likely that patients partially learn the impact of the robotic assistance on their strides dynamic and adapt their control according to this newly acquired knowledge. Therefore, we expect that the true impact of the orthosis on the stride variability and persistence be between the results found with full adaptation and those found with no adaptation at all. Depending on the degree of adaptation of each patient, the level of assistance can be adjusted to obtain gait characteristics as close as possible to those of healthy population. Note that it is reasonable to assume that patients do adapt to the orthosis, at least partially, considering that Parkinson's patients adapt successfully their gait to split-belt treadmill [34]. This adaptation occurred within the first 50 strides [35]. Further research is needed to investigate whether and how quickly they can adapt to a robotic device.

As for healthy population, the model simulated the behavior of an average patient, under the assumption that a specific H&Y corresponds to a specific gait impairment given by the regression. For clinical applications, the level of assistance must be individualized according to the actual needs of each patient and their personal ability to adapt to the robotic assistance. The level of assistance of an orthosis based on adaptive oscillators such as the Active Pelvis Orthosis presented in [36] is set by a virtual stiffness parameter, which controls the torque to be provided to the user at the hip level. This parameter

also accounts for the patient's weight to guarantee a safe interaction.

The less flexible control strategy of patients could be ascribed in the model to a relative inability to exploit the GEM. This allows one to formulate the hypothesis that patients with PD might have an altered internal task formulation and fail to exploit the redundancy of the task, whereby a target velocity can be achieved with different combination of stride timing and amplitude. Support for this interpretation is given by current theories associating movement related costs and the basal ganglia [37]. This idea was supported by the work of Mazzoni and colleagues [38], who showed that movement slowing in PD could not be attributed to an inability to execute accurate movements. Indeed, patients demonstrated normal speed-accuracy tradeoffs compared to the performance of healthy subjects, but they were more reluctant to perform fast movements (i.e. they needed more trials to reach the correct velocity). It was suggested that patients may associate an abnormally high cost for movements that they are otherwise able to execute. Our present developments suggest that not only the value of the cost, but also its structure (in this case, the GEM) may not be well represented in this population.

The model provides a discrete characterization of gait in two different populations (healthy – patients) and conditions (assisted – unassisted). It is possible to connect this model with continuous time models [8], [10] and to leverage frameworks recently developed to recover joint forces and muscles activation to build a comprehensive musculoskeletal model [39], [40]. For exemple, as done in [8], the simulated series of stride frequency might be the input to a nonlinear forced Van der Pol oscillator whose output is the movement of the two legs. However, even if the resulting series of stride frequency slightly differ from the input frequencies, they keep the same fractal properties, mean and standard deviation.

One implicit hypothesis that motivated our investigation on the presence and recovery of statistical persistence in patients was the hope that restoring LRA could have a causal influence on fall risk. Indeed, the fractal exponent of strides series has been proposed to be a predictive marker of fall [41], although this remains uncertain. Indeed, the loss of persistence might not be the cause of fall risk, but rather a marker of the compensatory mechanism, which is itself linked to disease severity and necessarily correlated with fall risk. We expect that future research will address this issue in details.

To summarise, the model developed to simulate gait variability of patients with Parkinson's disease suggested that these patients adopted a control strategy that sought to strictly regulate the deviation from the preferred target stride duration and length, in addition to the coordinated regulation of stride velocity. This strategy could be initiated to limit the increased stride variability that characterizes Parkinson's disease and makes patients' gait less stable. As a consequence of this less flexible control, the variability of their series of inter-stride durations displays a reduced level of autocorrelation, a marker of reduced adaptive capabilities and higher risk of falling. In addition, this study predicts an improvement in both the stride durations variability and statistical persistence for patients assisted with an oscillator-based robotic device. We believe that our modelling work provides a strong theoretical ground for future investigations on the benefit of gait assistance technologies in clinical populations.

REFERENCES

[1] J. M. Hausdorff, C. K. Peng, Z. Ladin, J. Y. Wei, and A. L. Goldberger, "Is walking a random walk? Evidence for long-range correlations in stride interval of human gait," *J. Appl. Physiol.*, vol. 78, no. 1, pp. 349–358, Jan. 1995.

[2] G. Rangarajan and M. Ding, "Integrated approach to the assessment of long range correlation in time series data," *Phys. Rev. E, Stat. Phys. Plasmas Fluids Relat. Interdiscip. Top.*, vol. 61, no. 5, p. 4991, 2000.

[3] N. Stergiou and L. M. Decker, "Human movement variability, nonlinear dynamics, and pathology: Is there a connection?" *Hum. Movement Sci.*, vol. 30, no. 5, pp. 869–888, 2011.

[4] R. Bartsch, M. Plotnik, J. W. Kantelhardt, S. Havlin, N. Giladi, and J. M. Hausdorff, "Fluctuation and synchronization of gait intervals and gait force profiles distinguish stages of Parkinson's disease," *Phys. A, Stat. Mech. Appl.*, vol. 383, no. 2, pp. 455–465, Sep. 2007.

[5] J. M. Hausdorff, "Gait dynamics in Parkinson's disease: Common and distinct behavior among stride length, gait variability, and fractal-like scaling," *Chaos: Interdiscipl. J. Nonlinear Sci.*, vol. 19, no. 2, 2009, Art. no. 026113.

[6] T. Warlop et al., "Temporal organization of stride duration variability as a marker of gait instability in Parkinson's disease," *J. Rehabil. Med.*, vol. 48, no. 10, pp. 865–871, Nov. 2016.

[7] F. Dierick, C. Vandevoorde, F. Chantraine, O. White, and F. Buisseret, "Benefits of nonlinear analysis indices of walking stride interval in the evaluation of neurodegenerative diseases," *Hum. Movement Sci.*, vol. 75, Feb. 2021, Art. no. 102741.

[8] B. J. West and N. Scafetta, "Nonlinear dynamical model of human gait," *Phys. Rev. E, Stat. Phys. Plasmas Fluids Relat. Interdiscip. Top.*, vol. 67, no. 5, p. 10, May 2003.

[9] Y. Sarbaz, S. Gharibzadeh, F. Towhidkhah, M. Banaie, and A. Jafari, "A gray-box neural network model of Parkinson's disease using gait signal," *Basic Clin. Neurosci.*, vol. 2, no. 3, pp. 33–42, 2011.

[10] D. H. Gates, J. L. Su, and J. B. Dingwell, "Possible biomechanical origins of the long-range correlations in stride intervals of walking," *Phys. A, Stat. Mech. Appl.*, vol. 380, pp. 259–270, Jul. 2007.

[11] J. B. Dingwell, J. John, and J. P. Cusumano, "Do humans optimally exploit redundancy to control step variability in walking?" *PLoS Comput. Biol.*, vol. 6, no. 7, p. 14, Jul. 2010.

[12] J. M. Hausdorff, Y. Ashkenazy, C.-K. Peng, P. C. Ivanov, H. E. Stanley, and A. L. Goldberger, "When human walking becomes random walking: Fractal analysis and modeling of gait rhythm fluctuations," *Phys. A, Stat. Mech. Appl.*, vol. 302, nos. 1–4, pp. 138–147, Dec. 2001.

[13] T. B. Warlop, B. Bollens, F. Crevecoeur, C. Detrembleur, and T. M. Lejeune, "Dynamics of revolution time variability in cycling pattern: Voluntary intent can alter the long-range autocorrelations," *Ann. Biomed. Eng.*, vol. 41, no. 8, pp. 1604–1612, Aug. 2013.

[14] M. Capecci et al., "Clinical effects of robot-assisted gait training and treadmill training for Parkinson's disease. A randomized controlled trial," *Ann. Phys. Rehabil. Med.*, vol. 62, no. 5, pp. 303–312, Sep. 2019.

[15] V. Otlet and R. Ronsse, "Predicting the effects of oscillator-based assistance on stride-to-stride variability of Parkinsonian walkers," in *Proc. Int. Conf. Robot. Autom. (ICRA)*, May 2022, pp. 8090–8096.

[16] M. A. Riley, S. Bonnette, N. Kuznetsov, S. Wallot, and J. Gao, "A tutorial introduction to adaptive fractal analysis," *Frontiers Physiol.*, vol. 3, p. 371, Jan. 2012.

[17] J. H. Hollman, W. D. Lee, D. C. Ringquist, C. Taisey, and D. K. Ness, "Comparing adaptive fractal and detrended fluctuation analyses of stride time variability: Tests of equivalence," *Gait Posture*, vol. 94, pp. 9–14, May 2022. [Online]. Available: https://linkinghub.elsevier.com/retrieve/pii/S0966636222000534

[18] B. B. Mandelbrot and J. W. Van Ness, "Fractional Brownian motions, fractional noises and applications," *SIAM Rev.*, vol. 10, no. 4, pp. 422–437, Oct. 1968.

[19] C. Roume, S. Ezzina, H. Blain, and D. Delignières, "Biases in the simulation and analysis of fractal processes," *Comput. Math. Methods Med.*, vol. 2019, pp. 1–12, Dec. 2019.

[20] C. K. Peng, S. V. Buldyrev, S. Havlin, M. Simons, H. E. Stanley, and A. L. Goldberger, "Mosaic organization of DNA nucleotides," *Phys. Rev.*, vol. 49, no. 2, p. 1685, Feb. 1994. [Online]. Available: https://journals.aps.org/pre/abstract/10.1103/PhysRevE.49.1685

[21] J. Gao, J. Hu, and W.-W. Tung, "Facilitating joint chaos and fractal analysis of biosignals through nonlinear adaptive filtering," *PLoS ONE*, vol. 6, no. 9, Sep. 2011, Art. no. e24331. [Online]. Available: https://journals.plos.org/plosone/article?id=10.1371/journal.pone.0024331

[22] E. Todorov, "Stochastic optimal control and estimation methods adapted to the noise characteristics of the sensorimotor system," *Neural Comput.*, vol. 17, no. 5, pp. 1084–1108, May 2005. [Online]. Available: https://direct.mit.edu/neco/article/17/5/1084/6949/Stochastic-Optimal-Control-and-Estimation-Methods

[23] R. Ronsse, N. Vitiello, T. Lenzi, J. Van Den Kieboom, M. C. Carrozza, and A. J. Ijspeert, "Human–robot synchrony: Flexible assistance using adaptive oscillators," *IEEE Trans. Biomed. Eng.*, vol. 58, no. 4, pp. 1001–1012, Apr. 2011.

[24] P. Terrier, V. Turner, and Y. Schutz, "GPS analysis of human locomotion: Further evidence for long-range correlations in stride-to-stride fluctuations of gait parameters," *Hum. Movement Sci.*, vol. 24, no. 1, pp. 97–115, Feb. 2005.

[25] P. Terrier and O. Dériaz, "Persistent and anti-persistent pattern in stride-to-stride variability of treadmill walking: Influence of rhythmic auditory cueing," *Hum. Movement Sci.*, vol. 31, no. 6, pp. 1585–1597, Dec. 2012.

[26] K. Kozlowska, M. Latka, and B. J. West, "Significance of trends in gait dynamics," *PLOS Comput. Biol.*, vol. 16, no. 10, Oct. 2020, Art. no. e1007180.

[27] J. M. Hausdorff, M. E. Cudkowicz, R. Firtion, F. Y. Wei, and A. L. Goldberger, "Gait variability and basal ganglia disorders: Stride-to-stride variations of gait cycle timing in Parkinson's disease and Huntington's disease," *Movement Disorders*, vol. 13, no. 3, pp. 428–437, 1998.

[28] K. Takakusaki, "Functional neuroanatomy for posture and gait control," *J. Movement Disorders*, vol. 10, no. 1, pp. 1–17, Jan. 2017.

[29] K. Baker, L. Rochester, and A. Nieuwboer, "The effect of cues on gait variability—Reducing the attentional cost of walking in people with Parkinson's disease," *Parkinsonism Related Disorders*, vol. 14, no. 4, pp. 314–320, May 2008.

[30] M. E. Morris, "Movement disorders in people with Parkinson disease: A model for physical therapy," *Phys. Therapy*, vol. 80, no. 6, pp. 578–597, Jun. 2000. [Online]. Available: https://academic.oup.com/ptj/article/80/6/578/2842508

[31] G. Yogev, N. Giladi, C. Peretz, S. Springer, E. S. Simon, and J. M. Hausdorff, "Dual tasking, gait rhythmicity, and Parkinson's disease: Which aspects of gait are attention demanding?" *Eur. J. Neurosci.*, vol. 22, no. 5, pp. 1248–1256, Sep. 2005.

[32] M. J. Hove, K. Suzuki, H. Uchitomi, S. Orimo, and Y. Miyake, "Interactive rhythmic auditory stimulation reinstates natural 1/f timing in gait of Parkinson's patients," *PLoS ONE*, vol. 7, no. 3, 2012, Art. no. 32600. [Online]. Available: https://www.plosone.org

[33] H. Uchitomi, L. Ota, K.-I. Ogawa, S. Orimo, and Y. Miyake, "Interactive rhythmic cue facilitates gait relearning in patients with Parkinson's disease," *PLoS ONE*, vol. 8, no. 9, Sep. 2013, Art. no. e72176. [Online]. Available: https://journals.plos.org/plosone/article?id=10.1371/journal.pone.0072176

[34] R. T. Roemmich, N. Hack, U. Akbar, and C. J. Hass, "Effects of dopaminergic therapy on locomotor adaptation and adaptive learning in persons with Parkinson's disease," *Behavioural Brain Res.*, vol. 268, pp. 31–39, Jul. 2014.

[35] F. Mohammadi et al., "Motor switching and motor adaptation deficits contribute to freezing of gait in Parkinson's disease," *Neurorehabil. Neural Repair*, vol. 29, no. 2, pp. 132–142, Mar. 2015, doi: 10.1177/1545968314545175.

[36] N. D'Elia et al., "Physical human–robot interaction of an active pelvis orthosis: Toward ergonomic assessment of wearable robots," *J. Neuroeng. Rehabil.*, vol. 14, no. 1, pp. 1–14, Apr. 2017. [Online]. Available: https://link.springer.com/articles/10.1186/s12984-017-0237-y and https://link.springer.com/article/10.1186/s12984-017-0237-y

[37] R. Shadmehr and J. W. Krakauer, "A computational neuroanatomy for motor control," *Experim. Brain Res.*, vol. 185, no. 3, pp. 359–381, 2008.

[38] P. Mazzoni, A. Hristova, and J. W. Krakauer, "Why don't we move faster? Parkinson's disease, movement vigor, and implicit motivation," *J. Neurosci.*, vol. 27, no. 27, pp. 7105–7116, Jul. 2007.

[39] I. Eskinazi and B. J. Fregly, "A computational framework for simultaneous estimation of muscle and joint contact forces and body motion using optimization and surrogate modeling," *Med. Eng. Phys.*, vol. 54, pp. 56–64, Apr. 2018.

[40] F. De Groote, A. L. Kinney, A. V. Rao, and B. J. Fregly, "Evaluation of direct collocation optimal control problem formulations for solving the muscle redundancy problem," *Ann. Biomed. Eng.*, vol. 44, no. 10, pp. 2922–2936, Oct. 2016.

[41] J. M. Hausdorff, "Gait dynamics, fractals and falls: Finding meaning in the stride-to-stride fluctuations of human walking," *Hum. Movement Sci.*, vol. 26, no. 4, pp. 555–589, 2007.